Marine Environmental Research 133 (2018) 15–23

Contents lists available at ScienceDirect

Marine Environmental Research

journal homepage: www.elsevier.com/locate/marenvrev

Physiological response of a red tide alga (*Skeletonema costatum*) to nitrate enrichment, with special reference to inorganic carbon acquisition

Guang Gao[a,b], Jianrong Xia[a,*], Jinlan Yu[a], Xiaopeng Zeng[a]

[a] School of Environmental Science and Engineering, Guangzhou University, Guangzhou 510006, China
[b] Marine Resources Development Institute of Jiangsu, Huaihai Institute of Technology, Lianyungang 222005, China

ARTICLE INFO

Keywords:
Carbonic anhydrase
CO_2 concentrating mechanisms
pH compensation point
Photosynthesis
Redox activity
Respiration

ABSTRACT

A classical red tide alga *Skeletonema costatum* was cultured under various nitrate levels to investigate its physiological response to nitrate enrichment combined with CO_2 limitation. The higher nitrate levels increased content of photosynthetic pigments (Chl *a* and Chl *c*), electron transport rate in photosystem II, photosynthetic O_2 evolution, and thus growth rate in *S. costatum*. On the other hand, the lower CO_2 levels (3.5–4.4 μmol kg^{-1} seawater) and higher pH (8.56–8.63) values in seawater were observed under higher nitrate conditions. Redox activity of plasma membrane and carbonic anhydrase in *S. costatum* was enhanced to address the reduced CO_2 level at higher nitrate levels. In addition, the pH compensation point was enhanced and direct HCO_3^- use was induced at higher nitrate levels. These findings indicate that nitrate enrichment would stimulate the breakout of *S. costatum* dominated red tides via enhancing its photosynthetic performances, and maintain a quick growth rate under CO_2 limitation conditions through improving its inorganic carbon acquisition capability. Our study sheds light on the mechanisms of *S. costatum* defeating CO_2 limitation during algal bloom.

1. Introduction

Diatoms is the most abundant and diverse group of phytoplanktonic eukaryote species (Simon et al., 2009). Marine diatoms contribute to approximately 20% of global primary production and 75% of the primary productivity for coastal and other nutrient-rich zones (Nelson et al., 1995; Field et al., 1998; Falkowski, 2012), hence playing a vital role in marine biological pump and regulating global climate change (Young and Morel, 2015). Although the concentration of dissolved inorganic carbon (DIC) is relative high (approximately 2 mmol L^{-1}) in seawater, CO_2 usually accounts for less than 1% of it, with the predominant form of HCO_3^-. This suggests CO_2 concentration in the seawater is far from saturating (> 50 μM) for diatoms' ribulose-1,5-bisphosphate carboxylase/oxygenase (Rubisco), the CO_2-fixing enzyme in the Calvin-Benson cycle (Hopkinson and Morel, 2011). To deal with the CO_2 limitation in seawater and maintain a high photosynthetic rate under changing carbon chemistry environments, diatoms have developed multiple inorganic carbon acquisition pathways, such as numerous carbonic anhydrases, active transport of HCO_3^-, unconventional C4 pathways, etc. (Hopkinson and Morel, 2011; Hopkinson et al., 2016).

Previous studies demonstrate that diatoms are generally more common in nutrient-rich systems (Irwin et al., 2012; Barton et al., 2015, 2016), and can often dominate the phytoplankton communities and form large-scale blooms in well-mixed coastal and upwelling regions (Bruland et al., 2001; Anderson et al., 2008). Although the occurrence of diatom blooms could be regulated by multiple environmental factors, such as water temperature, light irradiance, and salinity, a direct connection between spreading coastal eutrophication and the worldwide algal bloom is compelling (Smetacek and Zingone, 2013; Jeong et al., 2015). When inorganic nutrient loads are high, diatoms usually have a quicker growth rate and out-compete other bloom algae, such as dinoflagellates, raphidophytes and chrysophytes (Berg et al., 1997; Macintyre et al., 2004; Hu et al., 2011; Jeong et al., 2015; Barton et al., 2016).

Nitrogen is an essential nutrient for all organisms in terms of the biosynthesis of macromolecules, such as proteins, nucleic acids, and chlorophyll. Due to low availability, nitrogen is commonly considered as a major nutrient in limiting primary production in the worldwide oceans (Elser et al., 2007; Müller and Mitrovic, 2015). Extensive studies have been carried out to investigate the effect of nitrate on nitrogen uptake, utilization (Serra, 1978; Cochlan et al., 2008; Jauffrais et al., 2016), and nitrogen metabolism in diatoms (Allen et al., 2005, 2011; Brown et al., 2009; Kamp et al., 2016). However, little is known the effect of nitrate on inorganic carbon acquisition in diatoms, particularly under CO_2 limitation conditions.

* Corresponding author.
E-mail address: jrxia@gzhu.edu.cn (J. Xia).

https://doi.org/10.1016/j.marenvres.2017.11.003
Received 3 September 2017; Received in revised form 11 November 2017; Accepted 12 November 2017
Available online 14 November 2017
0141-1136/

S. costatum is a cosmopolitan diatom species that can be found in both coastal and open ocean areas. In coastal waters and estuaries where eutrophication can often occur, *S. costatum* is usually the most abundant algal species and dominate large-scale algal blooms (Wang, 2002; Li et al., 2011), influencing the biogeochemical cycling of carbon, silicon, and nitrogen, as well as ecosystem structure. Compared to other algae, *S. costatum* may experience more severe CO_2 limitation when bloom occurs. Accordingly, it has evolved multiple inorganic acquisition pathways and efficient CCMs (Nimer et al., 1998; Rost et al., 2003; Chen and Gao, 2004a). Nimer et al. (1998) found that extracellular carbonic anhydrase activity in *S. costatum* was induced when CO_2 concentration was less than 5 μmol L^{-1} and the induced CA could ensure that the photosynthetic carbon fixation was not affected by the decreasing CO_2 concentration. Rost et al. (2003) reported that activity of extracellular CA increased with decreasing pCO_2 (1800 − 36 μatm) and *S. costatum* could take up both CO_2 and HCO_3^- for photosynthesis and half saturation concentrations ($K_{1/2}$) of DIC for photosynthetic O_2 evolution declined with decreasing CO_2 concentration. On the other hand, Chen and Gao (2004a) demonstrated that this alga had poor capacity for direct HCO_3^- utilization and photosynthetic CO_2 affinity was regulated by the concentration of CO_2 rather than total dissolved inorganic carbon (DIC), HCO_3^-, or CO_3^{2-}.

Until now, most studies regarding inorganic carbon acquisition in *S. costatum* focus on its response to changes of CO_2 level. In regard to nitrate, it has been reported that nitrate enrichment could enhance the photosynthetic rate and growth in *S. costatum* (Smith et al., 1992; Liu et al., 2012), which may be attributed to the increased mRNA content of Rubisco (Liu et al., 2012) and nitrogen assimilation (Smith et al., 1992). However, the effect of nitrate enrichment on *S. costatum*'s photosynthetic performances, particularly inorganic carbon acquisition, under CO_2 limitation conditions, remains unclear. Based on the connections between nitrogen and carbon metabolisms in microalgae (Guerra et al., 2013; Fields et al., 2014), we hypothesize that nitrate enrichment could improve the capacity of inorganic carbon utilization and hence maintain high rates of photosynthesis and growth in *S. costatum* under CO_2 limitation conditions. In this study, we investigated the variation of inorganic acquisition pathways, photosynthetic CO_2 affinity, carbonic anhydrase activity, redox activity of plasma membrane, photosynthetic rate, and growth under various nitrate and CO_2 conditions to test this hypothesis. Our study would shed light on the potential mechanism that how bloom-forming diatoms maintain quick growth under CO_2 limitation conditions during red tides.

2. Materials and methods

2.1. Culture conditions

S. costatum (Grev.) Cleve from Jinan University, China, was cultured in 400 mL of artificial seawater enriched with f/2 medium free of nitrate at 20 °C for seven days and the initial cell concentration was 3.7×10^4 mL^{-1}. Five nitrate levels (1, 5, 25, 100, 200 μmol L^{-1}) were set in the artificial seawater by adding different amounts of $NaNO_3$. The nitrate concentrations in seawater were monitored daily by a spectrophotometer method (Collos et al., 1999). Batch cultures were conducted to mimic the process of red tides, cell concentration increasing and nutrient decreasing with time. The cultures were bubbled with ambient air at a rate of 100 mL min^{-1} to mimic the seawater mixing in the field. The light intensity was 200 μmol m^{-2} s^{-1} with a photoperiod of 12L: 12D. The light intensity of 200 μmol m^{-2} s^{-1} is saturated for *S. costatum*'s growth based on a preliminary experiment and also comparable to the literature on *S. costatum*'s inorganic carbon acquisition (Nimer et al., 1998; Chen and Gao, 2004a). The cells were collected during the exponential growth phase to conduct the following experiments. All experiments were conducted in triplicates.

2.2. Carbonate chemistry

The seawater pH was monitored with a pH meter (pH 700, Eutech Instruments, Singapore) and the total alkalinity (TA) was measured by titrations at 5:00 p.m. every day. The other carbonate system parameters, which were not directly measured, were calculated via CO2SYS (Pierrot et al., 2006), using the equilibrium constants of K1 and K2 for carbonic acid dissociation (Roy et al., 1993) and the KSO_4^- dissociation constant from Dickson (1990).

2.3. Growth estimation

Cell density was determined at 5:30 p.m. daily by direct counting with an improved Neubauer haemocytometer (XB-K-25, Qiu Jing, Shanghai, China). Specific growth rate (SGR) was determined from the changes in the cell density over the culture period as:

$$SGR = \ln (D_n/D_{n-1}) (t_n - t_{n-1})^{-1}$$

where D_n and D_{n-1} represent the cell densities at time t_n and t_{n-1}, respectively.

2.4. Chlorophyll fluorescence measurement

The relative ETR (rETR) was measured using a pulse modulation fluorometer (PAM-2100, Walz, Germany). The measuring light and actinic light were 0.01 and 200 μmol photons m^{-2} s^{-1}, respectively. The saturating pulse was set 4000 μmol photons m^{-2} s^{-1} (0.8 s). rETR (μmol e^- m^{-2} s^{-1}) = $(F_m' - F_t)/F_m' \times 0.5 \times$ PFD, photochemical quenching (q_p) = $(F_m' - F_t)/(F_m' - F_o)$, non-photochemical quenching (q_N) = $(F_m - F_m')/(F_m - F_o')$, where F_m' and F_m are the maximal fluorescence levels from algae after in light and dark adaptation (10 min), respectively. F_t is the fluorescence at an excitation level. Modulated (4 Hz) blue light and far-red light measuring beams were used to measure F_0 and F_0', respectively. PFD is the actinic light density.

2.5. Estimation of photosynthetic oxygen evolution

The net photosynthetic rate of *S. costatum* was measured by a Clark-type oxygen electrode (YSI Model 5300, USA) that was held in a circulating water bath (Cooling Circulator; Cole Parmer, Chicago, IL, USA) to keep the target temperature. Five mL of samples were transferred to the oxygen electrode cuvette and were stirred during measurement. The light intensity and temperature were maintained as the same as that in the growth condition. The illumination was provided by a halogen lamp. The increase of oxygen content in seawater within five minutes was defined as net photosynthetic rate. To measure dark respiration rate, the samples were placed in darkness and the decrease of oxygen content within ten minutes was defined as dark respiration rate. Net photosynthetic rate and dark respiration rate were presented as μmol O_2 $(10^9$ cells$)^{-1}$ h^{-1}.

To obtain the curve of net photosynthetic rate versus DIC, seven levels of DIC (0, 0.1, 0.2, 0.5, 1, 2, and 3 mM) were prepared by adding different amounts of $NaHCO_3$ to the Tris buffered DIC-free seawater. DIC was removed from the natural seawater by reducing pH to approximately 3.0 with the addition of 1.0 M HCl and sparging for 2 h with pure N_2 gas (99.999%). Finally, Tris buffer (25 mM) was added and the pH was adjusted to 8.2 with freshly prepared 1 M NaOH and 1 M HCl. The algal samples were washed twice with DIC-free seawater before transferring to the various DIC solutions. Photosynthetic rates at different DIC levels were measured under saturating irradiance of 400 μmol photons m^{-2} s^{-1} and growth temperature. The algal samples were allowed to equilibrate for 2–3 min at each DIC level during which period a linear change in oxygen concentration was obtained and recorded. The parameters, maximum photosynthetic rate (V_{max}), and the half saturation constant ($K_{0.5}$, i.e., the DIC concentration required to

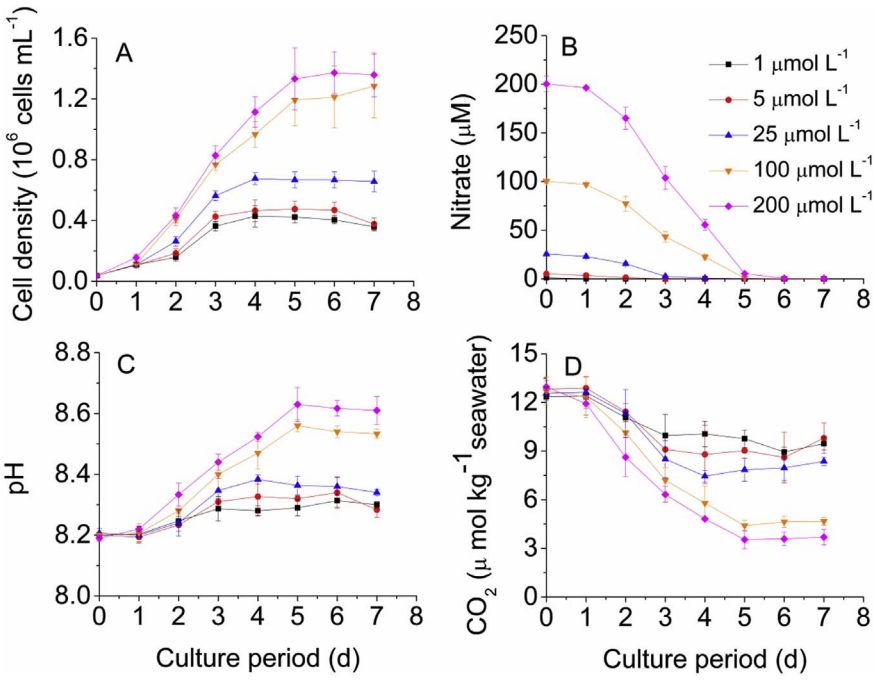

Fig. 1. Variation of cell density (A), nitrate (B), pH (C), and CO_2 (D) under various nitrate conditions over the culture period. The error bars indicate the standard deviations (n = 3).

give half of Ci-saturated maximum rate of photosynthetic O_2 evolution), were calculated from the Michaelis-Menten kinetics equation: $V = V_{max} \times [S]/(K_{0.5} + [S])$, where V is the photosynthetic rate and [S] is the DIC concentration.

2.6. Measurement of photosynthetic pigment

To determine the photosynthetic pigment (Chl *a* and Chl *c*) content, 50 mL of culture were filtered on a Whatman GF/F filter, extracted in 5 mL of 90% acetone for 12 h at 4 °C, and centrifuged (3, 000 *g*, 5 min). The optical density of the supernatant was scanned from 200 to 700 nm with a UV-VIS spectrophotometer (Shimadzu UV-1800, Kyoto, Japan). The concentrations of Chl *a* and Chl c were calculated based on the optical density at 630 and 664 nm: Chl $a = 11.47 \times OD_{664} - 0.40 \times OD_{630}$, Chl $c = 24.36 \times OD_{630} - 3.73 \times OD_{664}$.

2.7. Measurement of extracellular carbonic anhydrase activity

CA activity was assayed using the electrometric method of Gao et al. (2009). Cells were harvested by centrifugation at 4, 000 *g* for 5 min at 20 °C, washed once and resuspended in 8 mL Na-barbital buffer (20 mM, pH 8.2). Five mL CO_2-saturated icy pure was injected into the cell suspension, and the time required for a pH decrease from 8.2 to 7.2 at 4 °C was recorded. Extracellular and total CA activities were measured using intact cells and homogenized crude extracts, respectively. Intracellular CA activity (CAint) was determined as the difference between the total and extracellular CA activities (CAext). CA activity (E.U.) was calculated using the following formula: $E.U. = 10 \times (T_0/T - 1)$, where T_0 and T represent the time required for the pH change in the absence or presence of the samples, respectively.

2.8. Measurement of redox activity in the plasma membrane

The redox activity of plasma membrane was assayed by incubating the cells with 500 μmol ferricyanide [$K_3Fe(CN)_6$] that cannot penetrate intact cells and has been used as an external electron acceptor (Nimer et al., 1998). Stock solutions of $K_3Fe(CN)_6$ were freshly prepared before use. 5 mL of samples were taken from each nitrate treatment after 2 h of incubation with $K_3Fe(CN)_6$ and centrifuged at 4000 g for 10 min (20 °C). The absorbance of supernatant at 420 nm was measured immediately to assess the concentration of $K_3Fe(CN)_6$ and the difference between initial and final concentrations were used to calculate the rate of exofacial ferricyanide reduction (Nimer et al., 1998).

2.9. pH drift experiment

To obtain the pH compensation point, the cells were transferred to sealed glass vials containing fresh medium (pH 8.2) with corresponding nitrate levels. The cell concentration for all treatments was 3×10^5 mL^{-1}. The pH drift of the suspension was monitored at 20 °C and 200 μmol photons m^{-2} s^{-1} light level. The pH compensation point was obtained when there was no a further increase in pH (Chen and Gao, 2004a). After the last pH measurement, the algal sample was removed and the pH and alkalinity were measured after re-equilibration with air to determine how much of the observed pH increase was caused by net withdrawal of CO_2 during carboxylation catalysed by Rubisco.

2.10. Statistical analysis

The results were expressed as means of replicates ± standard deviation. Data were analyzed using the software SPSS v.21. The data from each treatment conformed to a normal distribution (Shapiro-Wilk, $P > 0.05$) and the variances could be considered equal (Levene's test, $P > 0.05$). Repeated measures ANOVAs were conducted to analyze the changes of cell density, nitrate concentration, pH and CO_2 concentration with culture time, the effects of DIC on net photosynthetic rate, and the effect of incubation time on media pH in a closed system. Bonferroni was conducted for *post hoc* investigation. One-way ANOVAs were conducted to assess the significant differences in specific growth rate, rETR, q_P, q_N, net photosynthetic rate, dark respiration rate, Chl *a*, Chl *c*, $V_{max,0.5}$, CA_{ext}, CA_{int}, reduction rate of ferricyanide, and pH compensation point among nitrate concentrations. Tukey HSD was conducted for *post hoc* investigation. Multivariate ANOVAs (MANOVAs) were conducted to analyze the difference between Chl *a* and Chl *c*, and between CA_{ext} and CA_{int} under each nitrate condition. The threshold value for determining statistical significance was $P < 0.05$.

3. Results

3.1. Changes of cell density and chemical conditions in the culture

The changes of cell density (Fig. 1A), nitrate concentration (Fig. 1B), pH (Fig. 1C), and CO_2 concentration (Fig. 1D) under different culture conditions were monitored over the culture period. Cell densities varied with culture time ($F_{(7, 70)} = 342.046$, $P < 0.001$) and the patterns under various nitrate conditions were different ($F_{(28, 70)} = 23.414$, $P < 0.001$). Specifically, *post hoc* Bonferroni comparison ($P = 0.05$) showed that cells cultured at nitrate levels of 1–25 μmol L^{-1} stopped growing and approached stationary phase by day 4 while those culture at 100 and 200 μmol L^{-1} nitrate continued to proliferate until day 5. Contrary to cell density, the nitrate levels in seawater decreased with culture time ($F_{(7, 70)} = 956.423$, $P < 0.001$). Nitrate concentrations under the conditions of 100 and 200 μmol L^{-1} nitrate reduced to zero by day 5 and those under the conditions of below 100 μmol L^{-1} nitrate were exhausted by day 3. The increase of cell density led to the rising of seawater pH with culture time ($F_{(7, 70)} = 175.834$, $P < 0.001$). *Post hoc* Bonferroni comparison ($P = 0.05$) showed that pH reached the peak by day 4 for those under 1–25 mol L^{-1} nitrate and by day 5 for those under 100 and 200 μmol L^{-1} nitrate. It is worth noting that the maximum pH could be 8.56 ± 0.02 and 8.63 ± 0.06 for the conditions of 100 and 200 μmol L^{-1} nitrate, respectively. Along with the rising of pH, CO_2 levels in seawater decreased with culture time ($F_{(7, 70)} = 158.078$, $P < 0.001$) and the minimum CO_2 levels for the conditions of 100 and 200 μmol L^{-1} nitrate were 4.4 ± 0.3 and 3.5 ± 0.6 μmol kg^{-1} seawater, respectively.

Nitrate enrichment significantly affected the specific growth rate in *S. costatum* over the 7 days of culture ($F_{(4, 10)} = 128.262$, $P < 0.001$, Fig. 2). *Post hoc* Tukey HSD comparison ($P = 0.05$) showed that although the slight increase in nitrate concentration (from 1 to 5 μmol L^{-1}) did not stimulate the specific growth rate, moderate enrichment of nitrate (25 μmol L^{-1}) increased SGR by 27% compared to the lowest nitrate level. The SGR was increased by 23% when nitrate varied from 25 to 100 μmol L^{-1} but further increase in nitrate (200 μmol L^{-1}) did not affect the SGR.

3.2. Effects of nitrate on photosynthetic and respiratory performances

To investigate the potential mechanisms that *S. costatum* continued to growth under high pH and low CO_2 when nitrate was replete, the photosynthetic performances of cells during the exponential growth phase (day 2 for 1–25 μmol L^{-1} nitrate conditions and day 4 for 100 and 200 μmol L^{-1} nitrate conditions) were measured. In terms of rETR in PS II (Fig. 3A), nitrate had a main effect on it ($F_{(4, 10)} = 130.605$, $P < 0.001$). *Post hoc* Tukey HSD comparison ($P = 0.05$) showed that there was no significant difference in rETR between 1 and 5 μmol L^{-1} nitrate treatments but a nearly 5-fold increase was achieved when nitrate increased to 25 μmol L^{-1} compared to 1 μmol L^{-1}. The rETR further increased to 19.0 ± 4.2 μmol e^{-} m^{-2} s^{-1} when nitrate was 100 μmol L^{-1}. The rETR (22.7 ± 1.4 μmol e^{-} m^{-2} s^{-1}) at 200 μmol L^{-1} was not significantly different from that at 100 μmol L^{-1}. The q_P also increased with nitrate availability ($F_{(4, 10)} = 67.67$, $P < 0.001$), with lowest (0.21 ± 0.05) at 1 μmol L^{-1} and highest (0.74 ± 0.04) at 200 μmol L^{-1} nitrate (Fig. 3B). On the other hand, there was a declining trend in q_N with the rising of nitrate concentration ($F_{(4, 10)} = 34.739$, $P < 0.001$, Fig. 3C). It decreased from 0.97 ± 0.03 to 0.86 ± 0.03 when nitrate increased from 1 to 25 μmol L^{-1} and further to 0.66 ± 0.04 at 200 μmol L^{-1} nitrate (Tukey HSD, $P < 0.05$).

Nitrate also affected net photosynthetic rate ($F_{(4, 10)} = 73.396$, $P < 0.001$, Fig. 4A) and dark respiration rate ($F_{(4, 10)} = 35.460$, $P < 0.001$, Fig. 4B). *Post hoc* Tukey HSD comparison ($P = 0.05$) showed that there was no significant difference in the net photosynthetic rates between 1 and 5 or 5 and 25 μmol L^{-1} nitrate levels but afterwards the net photosynthetic rate increased with nitrate (25–200 μmol L^{-1}), with the highest of 107.65 ± 12.60 μmol O_2 (10^9 cells)$^{-1}$ h^{-1} at 200 μmol L^{-1} nitrate. The pattern of dark respiration rate was the same as net photosynthetic rate except for the insignificant difference between 100 and 200 μmol L^{-1} nitrate (Tukey HSD, $P = 0.193$).

The main photosynthetic pigments in *S. costatum* grown at various nitrate concentrations were also measured (Fig. 5). Nitrate treatment significantly affected both Chl *a* ($F_{(4, 10)} = 290.442$, $P < 0.001$) and Chl *c* ($F_{(4, 10)} = 169.429$, $P < 0.001$). Chl *a* content increased (0.05 ± 0.01–0.27 ± 0.01 pg $cell^{-1}$) with nitrate level (5–200 μmol L^{-1}) but there was no significant difference between 1 and 5 μmol L^{-1} nitrate (Tukey HSD, $P = 0.996$). The pattern of Chl *c* was similar to Chl *a*, with insignificant difference between 5 and 25 μmol L^{-1} nitrate (Tukey HSD, $P = 0.195$). The content of Chl *c* was much lower than Chl *a* under each nitrate level ($F_{(1, 4)} > 70.199$, $P < 0.01$).

To investigate the photosynthetic response of *S. costatum* grown at various nitrate levels to DIC variation, the net photosynthetic rates of cells exposure to seven levels of DIC were measured (Fig. 6). The outcome of Repeated measures ANOVAs showed that net photosynthetic rate in *S. costatum* grown at all nitrate conditions increased with DIC, with higher increase amplitudes at higher nitrate conditions ($F_{(24, 60)} = 76.420$, $P < 0.001$). For instance, the net photosynthetic rate at 1 μmol L^{-1} nitrate increased from 0 to 35.02 ± 2.90 μmol O_2 (10^9 cells)$^{-1}$ h^{-1} when DIC changed 0–3 mmol L^{-1} while it increased from 0 to 81.44 ± 3.20 μmol O_2 (10^9 cells)$^{-1}$ h^{-1} for 200 μmol L^{-1} nitrate.

As shown in Table 1, nitrate significantly affected V_{max} ($F_{(4, 10)} = 156.943$, $P < 0.001$) and $K_{0.5}$ for DIC ($F_{(4, 10)} = 13.135$, $P = 0.001$), CO_2 ($F_{(4, 10)} = 14.303$, $P < 0.001$) and HCO_3^- ($F_{(4, 10)} = 13.131$, $P = 0.001$). *Post hoc* Tukey HSD comparison ($P = 0.05$) showed that V_{max} increased with nitrate level (5–200 μmol L^{-1}) although the difference between 1 and 5 μmol L^{-1} was insignificant. The variation trends of $K_{0.5}$ for DIC, CO_2 and HCO_3^- were the same. The increase of nitrate to 25 μmol L^{-1} did not change $K_{0.5}$ but further addition of nitrate led to significant increase in $K_{0.5}$. There was no significant difference in $K_{0.5}$ between 100 and 200 μmol L^{-1} nitrate levels.

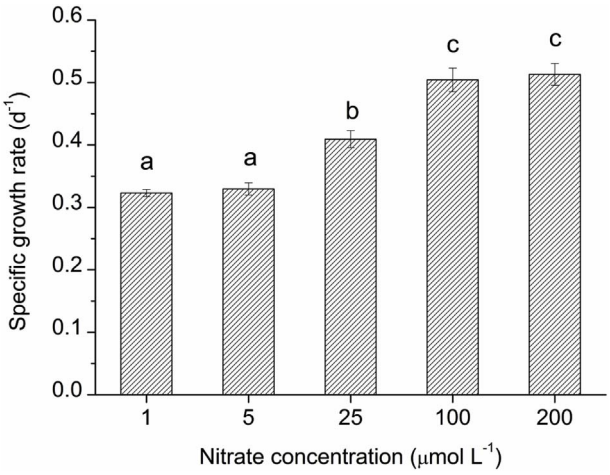

Fig. 2. Specific growth rates in *S. costatum* grown at various nitrate concentrations. The error bars indicate the standard deviations (n = 3). Different letters represent the significant difference ($P < 0.05$) among nitrate concentrations.

3.3. The response of inorganic carbon acquisition to CO_2 limitation and nitrate enrichment

To investigate the potential mechanism that cells combat CO_2 limitation under various nitrate conditions, the activity of CA_{ext} and CA_{int}

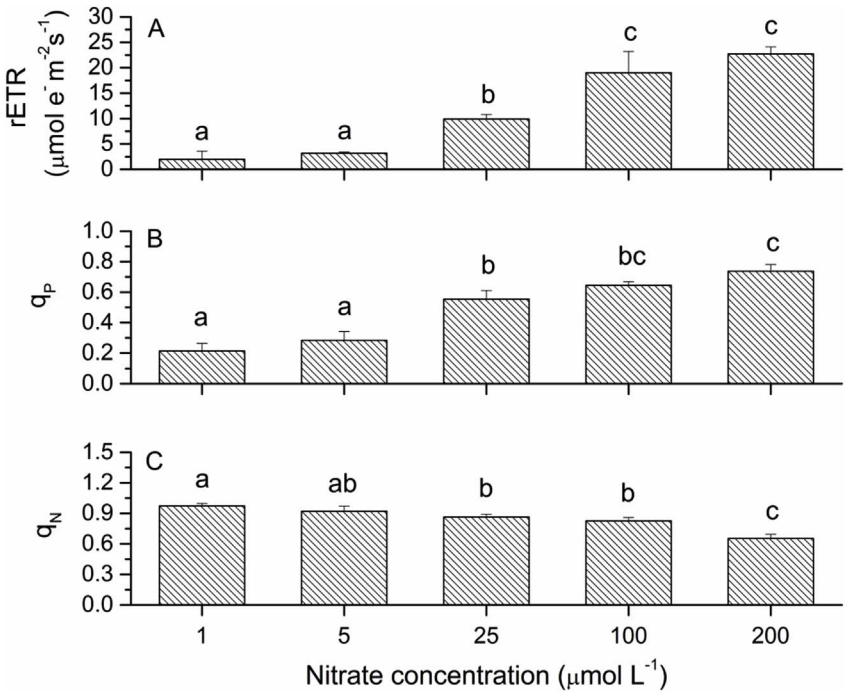

Fig. 3. Relative electron transport rate (rETR), photochemical quenching (q_P), and non-photochemical quenching (q_N) in *S. costatum* grown at various nitrate concentrations. The error bars indicate the standard deviations (n = 3). Different letters represent the significant difference ($P < 0.05$) among nitrate concentrations.

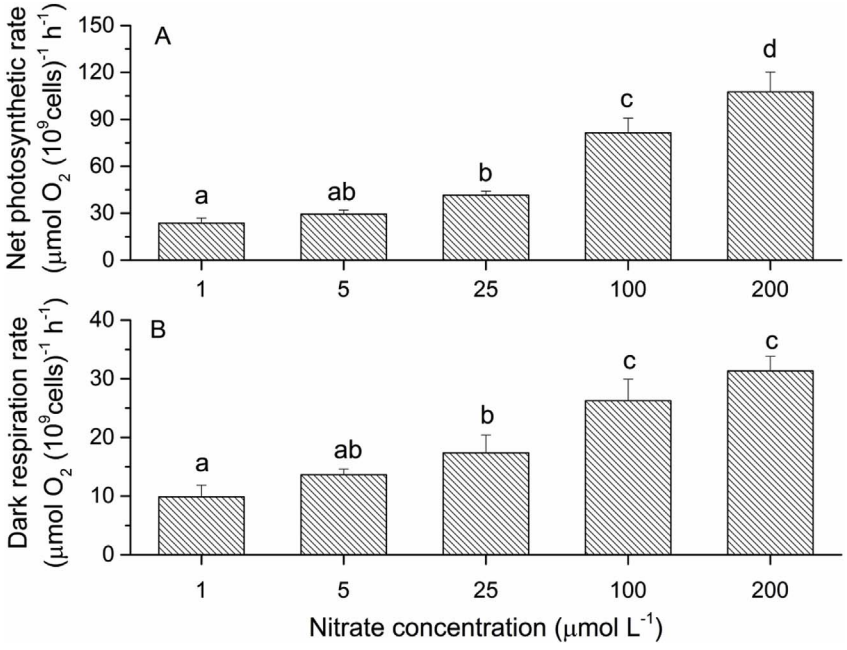

Fig. 4. Net photosynthetic rate (A) and dark respiration rate (B) in *S. costatum* grown at various nitrate concentrations. The error bars indicate the standard deviations (n = 3). Different letters represent the significant difference ($P < 0.05$) among nitrate concentrations.

were measured (Fig. 7A). There was a significant difference in CA_{ext} activity between nitrate levels ($F_{(4, 10)} = 747.861$, $P < 0.001$). *Post hoc* Tukey HSD comparison ($P = 0.05$) showed that 5 μmol L^{-1} nitrate did not increase CA_{ext} and afterwards CA_{ext} increased (0.048 ± 0.002–0.174 ± 0.004 EU $(10^6 \text{ cells})^{-1}$) with nitrate concentration (5–200 μmol L^{-1}). The trend of CA_{int} under various nitrate conditions was the same at CA_{ext}, with the lowest of at 0.012 ± 0.001 EU $(10^6 \text{ cells})^{-1}$ at 1 μmol L^{-1} nitrate and highest of 0.036 ± 0.002 EU $(10^6 \text{ cells})^{-1}$ at 200 μmol L^{-1}. CA_{int} was much lower than CA_{ext} under each nitrate condition ($F_{(1, 4)} > 516.674$, $P < 0.001$).

Nitrate also had a significant effect on the redox activity of plasma membrane ($F_{(4, 10)} = 243.956$, $P < 0.001$, Fig. 7B). *Post hoc* Tukey HSD comparison ($P = 0.05$) showed that the reduction rate of ferricyanide between 1 (14.77 ± 0.95 μmol $(10^6 \text{ cells})^{-1}$ h^{-1}) and 5 μmol L^{-1} nitrate (15.01 ± 2.19 μmol $(10^6 \text{ cells})^{-1}$ h^{-1}) was not significantly different and then it increased with nitrate availability, with the highest reduction rate (101.60 ± 7.36 μmol $(10^6 \text{ cells})^{-1}$ h^{-1}) at 200 μmol L^{-1} nitrate.

To obtain pH compensation points in *S. costatum* grown under various nitrate conditions, changes of pH in a closed system were monitored (Fig. 8). The pH in media under various nitrate conditions all increased with incubation time ($F_{(9, 90)} = 783.523$, $P < 0.001$) but they stopped at different points ($F_{(4, 10)} = 149.556$, $P < 0.001$). *Post hoc* Tukey HSD comparison ($P = 0.05$) showed that there was no significant difference in pH compensation point between 1 (8.84 ± 0.03) and 5 μmol L^{-1} (8.88 ± 0.02) nitrate. Then the pH compensation point increased with the rising of nitrate (5–200 μmol L^{-1}). The highest value of 9.22 ± 0.02 was obtained at 200 μmol L^{-1} nitrate. All of the

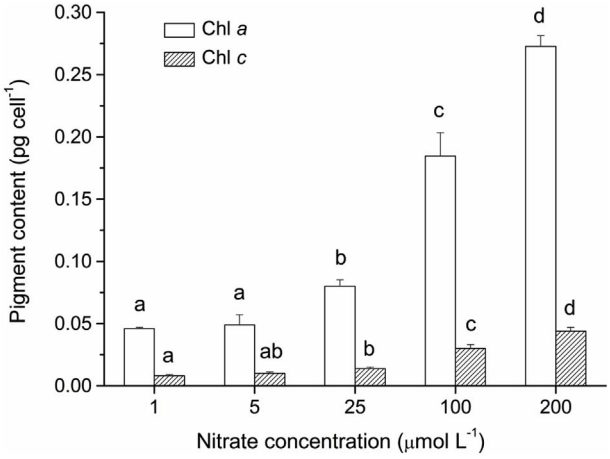

Fig. 5. Photosynthetic pigment content in *S. costatum* grown at various nitrate concentrations. The error bars indicate the standard deviations (n = 3). Different letters represent the significant difference ($P < 0.05$) in Chl *a* or Chl *c* among nitrate concentrations.

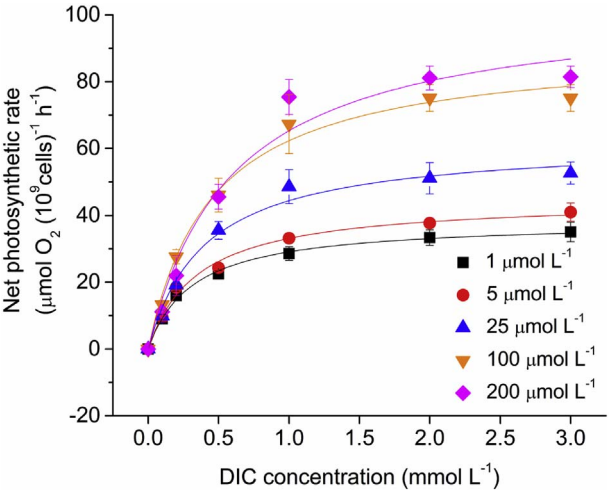

Fig. 6. Net photosynthetic rate as a function of DIC for *S. costatum* grown at various nitrate concentrations. The error bars indicate the standard deviations (n = 3).

pH change was due to photosynthetic CO_2 withdrawal as the measured pH and alkalinity after re-equilibration with air did not change compared to the initial values.

4. Discussion

4.1. Photosynthetic O_2 evolution

Nitrate can affect photosynthesis via multiple ways. Nitrogen starvation could cause a decline in thylakoid absorptivity (Plumley et al., 1989), lead to inactivation of PSII (Berges and Falkowski, 1996), and reduce photosynthetic pigments in microalgae (Donald et al., 2011). Higher nitrate increased photosynthetic pigments (Chl *a* and Chl *c*) of *S. costatum* in the present study, which is consistent with the previous studies on *S. costatum* (Davies and Sleep, 1989; Chen and Gao, 2004b). Nitrate enrichment commonly increases algal chlorophyll content due to its constitutive role in chlorophyll molecular (Geider et al., 1993; Donald et al., 2011). The increased photosynthetic pigments in *S. costatum* may contribute to the enhanced rETR, q_p, and net photosynthetic rate at higher nitrate levels.

4.2. CA activity and redox activity of plasma membrane

CA activity of *S. costatum* grown at higher nitrate levels was promoted in this study. Higher nitrate also induced higher CA activity in macroalgae *Ulva rigida* (Rio et al., 1995) and higher plant (Burnell et al., 1990; Makino et al., 1992) but little regarding microalgae has been documented. It has been reported that nitrogen could affect CA activity by regulating the expression of CA mRNA and the synthesis of CA protein (Burnell et al., 1990). In addition, the stimulating effect of nitrate on CA activity may be due to the carbon limit at higher nitrate conditions. CA activity of *S. costatum* grown at CO_2-replete conditions, i.e 2.0–3.0 mmol DIC and pH 8.2–8.3, is usually undetectable (Nimer et al., 1998) or very low (Gao et al., 2009) whilst CO_2 limitation can noticeably induce CA activity (Nimer et al., 1998; Chen and Gao, 2003). In the present study, increased biomass and photosynthetic rate in *S. costatum* at higher nitrate levels led to the increase of pH and decrease of CO_2 in spite of aeration. According to the previous studies on *S. costatum* (Nimer et al., 1998, 1999), the very low levels of CO_2 (3–4 μmol kg^{-1} seawater) under the conditions of 100 and 200 μmol L^{-1} nitrate in the present study could stimulate the CA activity.

Higher nitrate also resulted in increased redox activity of plasma membrane in *S. costatum*. This could be attributed to higher photosynthetic rates and thus greater CO_2 drawdown under higher nitrate conditions (Smith-Harding et al., 2017). It has been proposed that under CO_2 limitation conditions, superfluous reducing equivalents would be transported from the chloroplast into the cytosol (Heber, 1974) and thus support the redox chain in the plasma membrane (Rubinstein and Luster, 1993; Nimer et al., 1999). The redox chain could lead to protonation extrusion of active center of extracellular CA (Gautier et al., 1992; Nimer et al., 1998), which would activate the enzyme. Our results of increased redox activity of plasma membrane and CA activity combined with decreased CO_2 at higher nitrate levels support this hypothesis. Furthermore, the higher nitrate increased pigment content and hence ETR in PSII, which could generate excess reducing equivalents, particularly when CO_2 is severely limited. These excess reducing equivalents would trigger the redox activity of plasma membrane and CA activity.

Enhanced CA activity is usually a signal of up-regulation of CCM and would promote the inorganic carbon affinity of Rubisco (Wu et al., 2012; Gao and Campbell, 2014; Xu et al., 2017). However, increased CA activity and reduced inorganic carbon affinity were observed at

Table 1
Maximum photosynthetic rate (V_{max}) and the half saturation constant ($K_{0.5}$) in *S. costatum* grown at various nitrate concentrations. Different letters represent the significant difference ($P < 0.05$) among nitrate concentrations.

N concentration (μmol L^{-1})	V_{max} (μmol O_2 (10^9 cells)$^{-1}$ h^{-1})	$K_{0.5}$ (μM)		
		DIC	CO_2	HCO_3^-
1	38.35 ± 2.78^a	319.5 ± 11.6^a	2.4 ± 0.1^a	291.6 ± 10.6^a
5	44.90 ± 2.27^a	356.3 ± 28.2^a	2.7 ± 0.2^a	325.2 ± 25.8^a
25	62.08 ± 4.79^b	399.0 ± 8.2^{ab}	3.0 ± 0.1^{ab}	364.2 ± 7.5^{ab}
100	90.77 ± 4.39^c	460.2 ± 56.2^{bc}	3.5 ± 0.4^{bc}	420.0 ± 51.3^{bc}
200	104.11 ± 4.80^d	597.7 ± 97.1^c	4.5 ± 0.7^c	545.5 ± 88.6^c

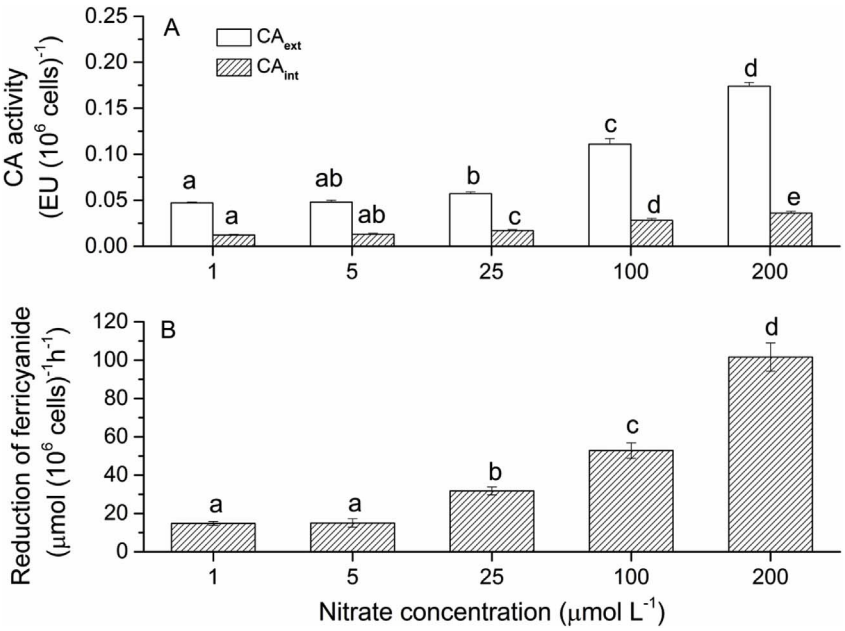

Fig. 7. CA activity (A) and reduction rate of ferricyanide (B) in *S. costatum* grown at various nitrate concentrations. The error bars indicate the standard deviations (n = 3). Different letters represent the significant difference ($P < 0.05$) in CA_{ext} or CA_{int} among nitrate concentrations.

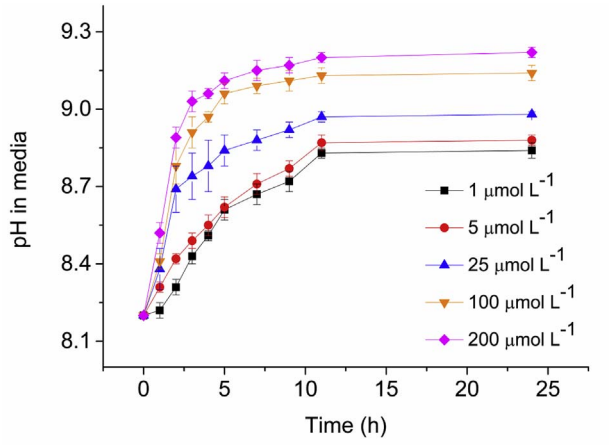

Fig. 8. Changes of pH in a closed system caused by photosynthesis of *S. costatum* grown at various nitrate concentrations. The error bars indicate the standard deviations (n = 3).

higher nitrate conditions in this study. Nitrate enrichment can promote the synthesis of Rubisco, as reported in *Phaeodactylum tricornutum* (Geider et al., 1993) and phytoplankton assemblages (Losh et al., 2013). Therefore, a possible reason for the contradiction between enhanced CA activity and decreased inorganic carbon affinity is that higher nitrate increased Rubisco content in *S. costatum* and hence more CO_2 was required to saturate Rubisco carboxylation. In addition, it was proposed that CCMs in algae grown under N limited conditions can be up-regulated to increase N-use efficiency and relieve N limitation (Beardall and Giordano, 2002; Raven et al., 2011). This could partially explain the increased inorganic carbon affinity at lower nitrate levels in the present study.

4.3. Direct HCO_3^- utilization

A pH compensation point over 9.2 has been deemed a sign of direct HCO_3^- use for algae, above which the higher the pH compensation point is; the stronger the ability to utilize HCO_3^- is (Axelsson and Uusitalo, 1988). For instance, red macroalgae, *Phycodrys rubens* and *Lomentaria articulata*, of which photosynthesis depends on CO_2 diffusion, have pH compensation points of less than 9.2 (Maberly, 1990). On the other hand, the marine diatom *Phaeodactylum tricornutum*, with strong capacity for direct HCO_3^- utilization, has a higher pH compensation point of 10.3 (Chen et al., 2006). In terms of *S. costatum*, it has been found to have a pH compensation point of 9.12, indicating a weak capacity for direct HCO_3^- utilization (Chen and Gao, 2004a). Our study demonstrates that nitrate available level could affect pH compensation point of *S. costatum*. The highest pH compensation point of 9.22 was achieved at 200 μmol nitrate level, suggesting that *S. costatum* could use HCO_3^- when nitrate is replete. Meanwhile, it is worth noting that minor conversion between HCO_3^- and CO_2 mediated by CAext may still occur at this pH based on the finding in *Chaetoceros muelleri* (Smith-Harding et al., 2017). Contrary to CO_2 passive diffusion, the direct use of HCO_3^- depends on positive transport that requires energy (Chen et al., 2006). The higher nitrate promoted the ETR in PSII in this study, from which the generated ATP could be used for HCO_3^- transport. In addition, the energy from the increased respiration at higher nitrate levels may also contribute to HCO_3^- transport. Our study indicates that nitrate enrichment could improve inorganic acquisition capacity of *S. costatum* to combat carbon limitation.

4.4. Growth and red tides

Diatoms usually dominate nutrient-rich coastal waters and estuaries (Li et al., 2011; Irwin et al., 2012; Barton et al., 2016) and *S. costatum* could outcompete other bloom algae (dinoflagellates *Prorocentrum minimum* and *Alexandrium tamarense*) via a quicker growth in nitrate and phosphate replete cultures (Hu et al., 2011). However, potential mechanisms are poorly understood. Our study demonstrates that nitrate enrichment could increase photosynthetic pigments and thus ETR and photosynthetic O_2 evolution. Furthermore, nitrate enrichment could promote CA activity and induce direct HCO_3^- use. This is particularly important, because pH in seawater could be very high during red tides along with extremely low CO_2 availability (Hansen, 2002; Hinga, 2002). For instance, pH level in the surface waters of the eutrophic Mariager Fjord, Denmark, is often above 9—occasionally up to 9.75 during dinoflagellate blooms (Hansen, 2002). The pH is relative low (8.63 ± 0.06) at the end of the seven days of batch culture even for the highest nitrate level in the present study. Although there was a large difference in initial nitrate concentration among treatments, the gap shrank with culture time and disappeared finally. This may explain the relative low cell density and thus low pH even at highest nitrate level. This relative low pH (8.63 ± 0.06) still led to a severe CO_2 limitation

(3.5 ± 0.6 μmol kg^{-1} seawater). The increased CA activity and induced direct HCO_3^- use under nitrate replete conditions would be helpful for *S. costatum* to overcome carbon limitation during algal bloom and to dominate red tides.

5. Conclusions

The present study investigated the potential mechanism that bloom-forming diatoms overcome CO_2 limitation and maintain a high growth rate during algal bloom for the first time. The fast growth of cells led to the increase of pH and decrease of CO_2 in the media. Cells grown at nitrate-depleted conditions entered into stationary phase whilst those at nitrate-replete conditions could continue to grow. The potential mechanism is that higher nitrate availability increased photosynthetic pigment content, ETR, and thus redox activity of plasma membrane and CA activity. In addition, higher nitrate availability induced direct HCO_3^- utilization that may be due to increased photosynthetic rate and ATP production. The increased CA activity and induced direct HCO_3^- use could ensure that *S. costatum* gets over carbon limitation over the algal bloom. This study provides important insight into the connection of nitrogen and carbon metabolisms in diatoms and the development of diatom-dominated red tides.

Acknowledgements

This work was supported by National Natural Science Foundation of China (No. 41376156 & 40976078), Natural Science Fund of Guangdong Province (No. S2012010009853), Jiangsu Planned Projects for Postdoctoral Research Funds (1701003A), Science and Technology Bureau of Lianyungang (SH1606), the Science Foundation of Huaihai Institute of Technology (Z2016007) and Foundation for High-level Talents in Higher Education of Guangdong.

References

Allen, A.E., Dupont, C.L., Oborník, M., Horák, A., Nunesnesi, A., Mccrow, J.P., Zheng, H., Johnson, D.A., Hu, H., Fernie, A.R., 2011. Evolution and metabolic significance of the urea cycle in photosynthetic diatoms. Nature 473 (7346), 203–207.

Allen, A.E., Ward, B.B., Song, B., 2005. Characterization of diatom (Bacillariophyceae) nitrate reductase genes and their detection in marine phytoplankton communities. J. Phycol. 41 (1), 95–104.

Anderson, D.M., Burkholder, J.M., Cochlan, W.P., Glibert, P.M., Gobler, C.J., Heil, C.A., Kudela, R., Parsons, M.L., Rensel, J.E., Townsend, D.W., 2008. Harmful algal blooms and eutrophication: examining linkages from selected coastal regions of the United States. Harmful Algae 8 (1), 39–53.

Axelsson, L., Uusitalo, J., 1988. Carbon acquisition strategies for marine macroalgae. Mar. Biol. 97 (2), 295–300.

Barton, A.D., Irwin, A.J., Finkel, Z.V., Stock, C.A., 2016. Anthropogenic climate change drives shift and shuffle in North Atlantic phytoplankton communities. Proc. Natl. Acad. Sci. U. S. A. 113 (11), 2964–2969.

Barton, A.D., Lozier, M.S., Williams, R.G., 2015. Physical controls of variability in North Atlantic phytoplankton communities. Limnol. Oceanogr. 60 (1), 181–197.

Beardall, J., Giordano, M., 2002. Ecological implications of microalgal and cyanobacterial CO_2 concentrating mechanisms, and their regulation. Funct. Plant Biol. 29 (3), 335–347.

Berg, G.M., Glibert, P.M., Lomas, M.W., Burford, M.A., 1997. Organic nitrogen uptake and growth by the chrysophyte *Aureococcus anophagefferens* during a brown tide event. Mar. Biol. 129 (2), 377–387.

Berges, J.A., Falkowski, P.G., 1996. Differential effects of nitrogen limitation on photosynthetic efficiency of photosystems I and II in microalgae. Plant Physiol. 110 (2), 689–696.

Brown, K.L., Twing, K.I., Robertson, D.L., 2009. Unraveling the regulation of nitrogen assimilation in the marine diatom *Thalassiosira pseudonana* (bacillariophyceae): diurnal variations in transcript levels for five genes involved in nitrogen assimilation. J. Phycol. 45 (2), 413–426.

Bruland, K.W., Rue, E.L., Smith, G.J., 2001. Iron and macronutrients in California coastal upwelling regimes: implications for diatom blooms. Limnol. Oceanogr. 46 (7), 1661–1674.

Burnell, J.N., Suzuki, I., Sugiyama, T., 1990. Light induction and the effect of nitrogen status upon the activity of carbonic anhydrase in maize leaves. Plant Physiol. 94 (1), 384–387.

Chen, X., Gao, K., 2003. Effect of CO_2 concentrations on the activity of photosynthetic CO_2 fixation and extracellular carbonic anhydrase in the marine diatom *Skeletonema costatum*. Chin. Sci. Bull. 48 (23), 2616–2620.

Chen, X., Gao, K., 2004a. Photosynthetic utilisation of inorganic carbon and its regulation in the marine diatom *Skeletonema costatum*. Funct. Plant Biol. 31 (10), 1027–1033.

Chen, X., Gao, K., 2004b. Response of photosynthesis of the bloom-forming marine diatom *Skeletonema costatum* to changes in pH and inorganic nitrogen concentrations in seawater. Acta Hydrobiol. Sin. 28 (6), 635–639.

Chen, X., Qiu, C.E., Shao, J.Z., 2006. Evidence for K^+-dependent HCO_3^- utilization in the marine diatom *Phaeodactylum tricornutum*. Plant Physiol. 141 (2), 731–736.

Cochlan, W.P., Herndon, J., Kudela, R.M., 2008. Inorganic and organic nitrogen uptake by the toxigenic diatom *Pseudo-nitzschia* australis (Bacillariophyceae). Harmful Algae 8 (1), 111–118.

Collos, Y., Mornet, F., Sciandra, A., Waser, N., Larson, A., Harrison, P.J., 1999. An optical method for the rapid measurement of micromolar concentrations of nitrate in marine phytoplankton cultures. J. Appl. Phycol. 11 (2), 179–184.

Davies, A.G., Sleep, J.A., 1989. The photosynthetic response of nutrient-depleted dilute cultures of *Skeletonema costatum* to pulses of ammonium and nitrate; the importance of phosphate. J. Plankton Res. 11 (1), 141–164.

Dickson, A.G., 1990. Standard potential of the reaction: AgCl(s) + 12H2(g) = Ag(s) + HCl(aq), and the standard acidity constant of the ion HSO_4^- in synthetic sea water from 273.15 to 318.15 K. J. Chem. Thermodyn. 22 (2), 113–127.

Donald, D.B., Bogard, M.J., Kerri, F., Leavitt, P.R., 2011. Comparative effects of urea, ammonium, and nitrate on phytoplankton abundance, community composition, and toxicity in hypereutrophic freshwaters. Limnol. Oceanogr. 56 (6), 2161–2175.

Elser, J.J., Bracken, M.E.S., Cleland, E.E., Gruner, D.S., Harpole, W.S., Hillebrand, H., Ngai, J.T., Seabloom, E.W., Shurin, J.B., Smith, J.E., 2007. Global analysis of nitrogen and phosphorus limitation of primary producers in freshwater, marine and terrestrial ecosystems. Ecol. Lett. 10 (12), 1135–1142.

Falkowski, P., 2012. Ocean Science: the power of plankton. Nature 483 (7387), 17–20.

Field, C.B., Behrenfeld, M.J., Randerson, J.T., Falkowski, P., 1998. Primary production of the biosphere: integrating terrestrial and oceanic components. Science 281 (5374), 237–240.

Fields, M.W., Hise, A., Lohman, E.J., Bell, T., Gardner, R.D., Corredor, L., Moll, K., Peyton, B.M., Characklis, G.W., Gerlach, R., 2014. Sources and resources: importance of nutrients, resource allocation, and ecology in microalgal cultivation for lipid accumulation. Appl. Microbiol. Biotechnol. 98 (11), 4805–4816.

Gao, G., Gao, K., Giordano, M., 2009. Responses to solar UV radiation of the diatom *Skeletonema costatum* (Bacillariophyceae) grown at different Zn^{2+} concentrations. J. Phycol. 45 (1), 119–129.

Gao, K., Campbell, D.A., 2014. Photophysiological responses of marine diatoms to elevated CO_2 and decreased pH: a review. Funct. Plant Biol. 41 (5), 449–459.

Gautier, H., Vavasseur, A., Lascève, G., Boudet, A.M., 1992. Redox processes in the blue light response of guard cell protoplasts of *Commelina communis* L. Plant Physiol. 98 (1), 34–38.

Geider, R.J., Roche, J.L., Greene, R.M., Olaizola, M., 1993. Response of the photosynthetic apparatus of *Phaeodactylum tricornutum* (bacillariophyceae) to nitrate, phosphate, or iron starvation. J. Phycol. 29 (6), 755–766.

Guerra, L.T., Levitan, O., Frada, M.J., Sun, J.S., Falkowski, P.G., Dismukes, G.C., 2013. Regulatory branch points affecting protein and lipid biosynthesis in the diatom *Phaeodactylum tricornutum*. Biomass Bioenergy 59 (1), 306–315.

Hansen, P.J., 2002. Effect of high pH on the growth and survival of marine phytoplankton: implications for species succession. Aquat. Microb. Ecol. 28 (3), 279–288.

Heber, U., 1974. Metabolite exchange between chloroplasts and cytoplasm. Ann. Rev. Plant Physiol. 25 (25), 393–421.

Hinga, K.R., 2002. Effects of pH on coastal marine phytoplankton. Mar. Ecol. Prog. Ser. 238, 281–300.

Hopkinson, B.M., Dupont, C.L., Matsuda, Y., 2016. The physiology and genetics of CO_2 concentrating mechanisms in model diatoms. Curr. Opin. Plant Biol. 31, 51–57.

Hopkinson, B.M., Morel, F.M.M., 2011. Efficiency of the CO_2-concentrating mechanism of diatoms. Proc. Natl. Acad. Sci. U. S. A. 108 (10), 3830–3837.

Hu, H., Zhang, J., Chen, W., 2011. Competition of bloom-forming marine phytoplankton at low nutrient concentrations. J. Environ. Sci-China 23 (4), 656–663.

Irwin, A.J., Nelles, A.M., Finkel, Z.V., 2012. Phytoplankton niches estimated from field data. Limnol. Oceanogr. 57 (3), 787–797.

Jauffrais, T., Jesus, B., Méléder, V., Turpin, V., Russo, A.D.A.P.G., Raimbault, P., Jézéquel, V.M., 2016. Physiological and photophysiological responses of the benthic diatom *Entomoneis paludosa* (Bacillariophyceae) to dissolved inorganic and organic nitrogen in culture. Mar. Biol. 163 (5), 115.

Jeong, H.J., An, S.L., Franks, P.J.S., Lee, K.H., Ji, H.K., Kang, N.S., Lee, M.J., Jang, S.H., Lee, S.Y., Yoon, E.Y., 2015. A hierarchy of conceptual models of red-tide generation: nutrition, behavior, and biological interactions. Harmful Algae 47, 97–115.

Kamp, A., Stief, P., Bristow, L.A., Thamdrup, B., Glud, R.N., 2016. Intracellular nitrate of marine diatoms as a driver of anaerobic nitrogen cycling in sinking aggregates. Front. Microbiol. 7, 1669.

Li, G., Gao, K., Yuan, D., Zheng, Y., Yang, G., 2011. Relationship of photosynthetic carbon fixation with environmental changes in the Jiulong River estuary of the South China Sea, with special reference to the effects of solar UV radiation. Mar. Pollut. Bull. 62 (8), 1852–1858.

Liu, Y., Song, X., Cao, X., Yu, Z., 2012. Responses of photosynthetic characters of *Skeletonema costatum* to different nutrient conditions. J. Plankton Res. 35 (1), 165–176.

Losh, J.L., Young, J.N., Morel, F.M., 2013. Rubisco is a small fraction of total protein in marine phytoplankton. New Phytol. 198 (1), 52–58.

Maberly, S.C., 1990. Exogenous sources of inorganic carbon for photosynthesis by marine macroalgae. J. Phycol. 26 (3), 439–449.

Macintyre, H.L., Lomas, M.W., Cornwell, J., Suggett, D.J., Gobler, C.J., Koch, E.W., Kana, T.M., 2004. Mediation of benthic–pelagic coupling by microphytobenthos: an energy- and material-based model for initiation of blooms of *Aureococcus anophagefferens*. Harmful Algae 3 (4), 403–437.

Makino, A., Sakashita, H., Hidema, J., Mae, T., Ojima, K., Osmond, B., 1992. Distinctive responses of ribulose-1,5-bisphosphate carboxylase and carbonic anhydrase in wheat leaves to nitrogen nutrition and their possible relationships to CO_2-transfer resistance. Plant Physiol. 100 (4), 1737–1743.

Müller, S., Mitrovic, S.M., 2015. Phytoplankton co-limitation by nitrogen and phosphorus in a shallow reservoir: progressing from the phosphorus limitation paradigm. Hydrobiologia 744 (1), 255–269.

Nelson, D.M., Tréguer, P., Brzezinski, M.A., Leynaert, A., Quéguiner, B., 1995. Production and dissolution of biogenic silica in the ocean: revised global estimates, comparison with regional data and relationship to biogenic sedimentation. Glob. Biogeochem. Cy 9 (3), 359–372.

Nimer, N.A., Ling, M.X., Brownlee, C., Merrett, M.J., 1999. Inorganic carbon limitation, exofacial carbonic anhydrase activity, and plasma membrane redox activity in marine phytoplankton species. J. Phycol. 35 (6), 1200–1205.

Nimer, N.A., Warren, M., Merrett, M.J., 1998. The regulation of photosynthetic rate and activation of extracellular carbonic anhydrase under CO_2-limiting conditions in the marine diatom *Skeletonema costatum*. Plant Cell Environ. 21 (8), 805–812.

Pierrot, D., Lewis, E., Wallace, D.W.R., 2006. MS Excel Program Developed for CO_2 System Calculations. ORNL/CDIAC-105a. Carbon Dioxide Information Analysis Center, Oak Ridge National Laboratory, US Department of Energy, Oak Ridge, Tennessee.

Plumley, F.G., Douglas, S.E., Switzer, A.B., Schmidt, G.W., 1989. Nitrogen-dependent biogenesis of chlorophyll-protein complexes. Plant Biol. 8, 311–329.

Raven, J.A., Giordano, M., Beardall, J., Maberly, S.C., 2011. Algal and aquatic plant carbon concentrating mechanisms in relation to environmental change. Photosynth. Res. 109 (1–3), 281–296.

Rio, M.J.D., Ramazanov, Z., Reina, G.G., 1995. Effect of nitrogen supply on photosynthesis and carbonic anhydrase activity in the green seaweed *Ulva rigida* (Chlorophyta). Mar. Biol. 123 (4), 687–691.

Rost, B., Riebesell, U., Burkhardt, S., Sültemeyer, D., 2003. Carbon acquisition of bloom-forming marine phytoplankton. Limnol. Oceanogr. 48 (48), 55–67.

Roy, R.N., Roy, L.N., Vogel, K.M., Porter-Moore, C., Pearson, T., Good, C.E., Millero, F.J., Campbell, D.M., 1993. The dissociation constants of carbonic acid in seawater at salinities 5 to 45 and temperatures 0 to 45°C. Mar. Chem. 44 (2–4), 249–267.

Rubinstein, B., Luster, D.G., 1993. Plasma membrane redox activity: components and role in plant processes. Annu. Rev. Plant Biol. 44 (1), 131–155.

Serra, J., 1978. Nitrate utilization by the diatom *Skeletonema costatum*. Plant Physiol. 62 (6), 987–990.

Simon, N., Cras, A.L., Foulon, E., Lemée, R., 2009. Diversity and evolution of marine phytoplankton. C. R. Biol. 332 (2–3), 159–170.

Smetacek, V., Zingone, A., 2013. Green and golden seaweed tides on the rise. Nature 504 (7478), 84–88.

Smith, G.J., Zimmerman, R.C., Alberte, R.S., 1992. Molecular and physiological responses of diatoms to variable levels of irradiance and nitrogen availability: growth of *Skeletonema costatum* in simulated upwelling conditions. Limnol. Oceanogr. 37 (5), 989–1007.

Smith-Harding, T.J., Beardall, J., Mitchell, J.G., 2017. The role of external carbonic anhydrase in photosynthesis during growth of the marine diatom Chaetoceros muelleri. J. Phycol. http://dx.doi.org/10.1111/jpy.12572.

Wang, J., 2002. Phytoplankton communities in three distinct ecotypes of the Changjiang estuary. J. Ocean. Univ. China 32, 422–428.

Wu, X., Gao, G., Giordano, M., Gao, K., 2012. Growth and photosynthesis of a diatom grown under elevated CO_2 in the presence of solar UV radiation. Fund. Appl. Limnol. 180, 279–290.

Xu, Z., Gao, G., Xu, J., Wu, H., 2017. Physiological response of a golden tide alga (*Sargassum muticum*) to the interaction of ocean acidification and phosphorus enrichment. Biogeosciences 14, 671–681.

Young, J.N., Morel, F.M.M., 2015. Biological oceanography: the CO_2 switch in diatoms. Nat. Clim. Change 5 (8), 722–723.